

Semesterarbeit in Neuroinformatics

An AVLSI-case study on the Self biasing Adaptive Photoreceptor

Daniel Oberhoff

March 27, 2003

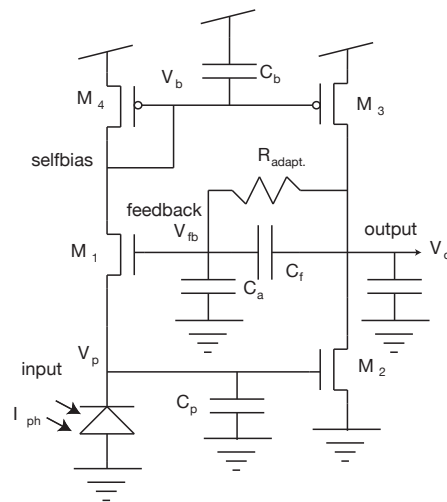


Figure 1: The Self biasing Adaptive Photoreceptor

Abstract

in this article I will review my semesterarbeit in the Institute of Neuroinformatics of the University of Zuerich Irchel. The task i had been given was to understand a certain circuit, the Self biasing Adaptive Photoreceptor which is an advanced version of the Adaptive Photoreceptor, both designed by Tobi Delbrueck who was also the supervisor of this Project, and to work out a theoretical model for it using small signal analysis.

I will then first explain the method of circuit analysis with small signals, apply it to three development stages of the circuit (the one in figure 1 and its predecessors) and try to explain the results in an intuitive fashion. I will also discuss stability and noise aspects within and beyond the scope of this method. I will then go on to not so intuitive numerical calculations and simulations and afterwards compare to the actual measurement.

Contents

1	Introduction	3
2	Circuit Analysis with Small Signals	4
2.1	CMOS integration	4
2.2	Prerequisites	4
2.3	Principles of the Analysis	4
2.4	Analysis of the Self biasing Adaptive Photoreceptor	6
2.5	Analysis of the Statically Biased Adaptive Photoreceptor	12
2.6	Simple source follower photoreceptor	13
2.7	Numerical analysis	15
2.8	Predictions for Stability and optimal tuning	16
2.9	Noise	17
3	Measurement	18
3.1	Stepresponses	18
3.1.1	Static bias	18
3.1.2	Adaptive Bias	18
3.2	Transfer function	19
3.3	Power consumption	19
4	Conclusion	20

1 Introduction

AVLSI is the study of integrated circuits containing large systems of purely analog circuitry. AVLSI makes explicit use of the intrinsically analog behavior of CMOS-technology. It thus rediscovers something one could call a lost art, as circuit design since the discovery of ICs has gone more and more in the direction of digital designs. Going in this direction one moves away from the actual physical behavior of the chip which is intrinsically analog and towards using more and more abstract metaphors and symbols which have meaning mainly in the use of the technology, but less in the implementation.

As the expectation for performance grows one reaches physical limits which are of analog nature. Within the digital paradigm this creates the need for implementation specialists providing new circuitry implementing the digital symbols. The AVLSI-paradigm on the other hand considers the analog behavior from the start and makes use of it, exploiting it as a possibility and not a limitation, strongly motivated by information processing in biological systems which in general is massively parallel, asynchronous and of course analog.

As will become clear in this text this is not an easy task! Even a seemingly simple circuit can generate a complexity in behavior and even chaotic behavior sometimes hardly feasible in its entirety. Thus most of the time one tries to keep the circuit in a certain domain of operation where certain theoretic approaches and simplifications can be successfully used.

The most widely used such method is the small signal analysis in which all the basic elements of the circuit under examination are subjected to a linear approximation. A Laplace Transform is then carried out (or equivalently an exponential Ansatz for the temporal evolution of all voltages in the system) which leads to a linear transfer function which in return can be used to predict frequency- and phase-response as well as step response and stability.

The circuit under examination here is the Self biasing Adaptive Photoreceptor conceptualized and implemented by Tobi Delbrueck. It is the successor of the Adaptive Photoreceptor, a circuit which makes logarithmic light intensity measurements without having the used photo diode driving the output (this task is carried out by a two-terminal inverting amplifier) and implementing (relatively) long term adaptation to steady state signals. Thus the measured signal is a measurement of the contrast to the actual signal to the steady state background level.

The new circuit implements another level of adaptation by scaling the reaction speed of the amplifier (which in reality is always finite) with the total incoming intensity (total within an array of these receptors on one chip). This way one reaches a self similar step-response scaling in time with the input intensity average over the light-sensitive of the chip. This means the chip exhibits the same behavior at low intensities as at high intensities, but on a longer time scale. This goes so far as integrating single photons hitting the diode to make up for a signal. Another advantage is that now the power consumption of the receptor scales also with intensity, thus this part of the chip will only consume power when it actually "sees" something, which is obviously very desirable.

The disadvantage of the new design is that under certain circumstances it exhibits unstable behavior. A motivation for this project was thus to understand the reasons for this behavior and to find recipes to avoid it. This goal has only been partially achieved. The models do predict a general instability for certain circuit parameters, in reality though it has been observed that the instability is present mainly at low light intensities, and this behavior could not be reconstructed in the models. Also to consider is that the statically biased circuit can be driven with a much higher bias than the self driven circuit and thus can be made to respond much faster and display less side effects like ringing while the self similarity and low power consumption are sacrificed.

2 Circuit Analysis with Small Signals

2.1 CMOS integration

The technology used for this circuit is Circuit Integration on a CMOS-IC custom and using a $1.5 \mu\text{m}$ process.

2.2 Prerequisites

To make a small signal analysis I need to know how the elements of the circuit behave and how the actual implementation on the chip influences this behavior. All the resources for this can be found in [2] and i will only review the relevant sections here.

As can be seen in the circuit diagram the Elements that make the circuit are Transistors and capacitors. The adaptive Element in the feedback path is a special device acting as a nonlinear resistor. The slope of the Current against the applied Voltage increases as one moves away from the axis, thus this element is said to have expansive characteristics. In practice this means that for small signals it can be left out of the analysis as its resistance is very high and thus the time scale of it charging and discharging the surrounding capacitances is much longer than any other relevant time scales. What it does is it will slowly adapt the charge on the feedback capacitor to a charge corresponding to the average output diminished by the capacitive divider ratio. In this situation the gain (including the negative feedback) is roughly the inverse of the capacitive divider ratio. Another way to picture this is seeing the charge on the feedback node as a model against which the input is compared, with the model being updated on a long term scale (low pass filtered) which results in a high pass filtered output (unfiltered minus low pass filtered).

2.3 Principles of the Analysis

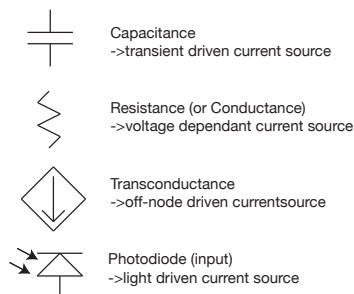


Figure 2: symbols used in the diagrammatical small signal analysis

Small signal analysis has been used for a long time and is thus well established. It follows a set of simple rules:

1. The Ansatz for all signals in the circuit made is: $V(t) = V_0 e^{st}$ where V can be any signal, current or voltage.
2. The equations for all involved elements are linearized about the circuits operating point (OP) by making a first order approximation (it is possible to still consider second order effects like the early effect in transistors through additional linear terms).

3. All temporal derivatives are now replaced by multiplication with s (this follows from the Ansatz, but can effectively leads to the same results that a Laplace-Transform would lead to, so effectively a Laplace-Transform is made).
4. All constant reference voltages are dropped from the equations since one is only interested in the actual signal, not the DC-background (the DC can still enter factors in the equation as a constant, which actually will simplify some of the equations). This is made clear by replacing all symbols for time varying voltage or current are replaced with small letters.

Also a System to diagrammatically represent the circuit has been established:

1. A diagram is made for every signal carrying node in the circuit (see figure 2).
2. All the Current inlets and outlets from and to that node are depicted referenced to ground with the first order term governing that current beside it.
3. A set of established symbols is used to represent these current sources (effectively 3 kinds of symbols: externally driven current sources, that is driven by another signal than the node voltage, resistors and capacitances; i deviate from this at the input node, the photo current, to distinguish it as the input node).

When i did the small signal analysis i didn't quite follow these rules through:

1. Wherever the voltage at the node corresponding to the diagram was driving a current source i didn't write it beside the element, making it easier for me to distinguish between externally driven currents and currents driven by that node (and effectively distinguish between conductances and transconductances).
2. In a second step I re normalized all currents and voltages so they would become dimensionless, usually by a dedicated Background current (DC) and the Thermal Voltages Respectively, and all the conductances by one dedicated one; when there are transistors that share a current or have currents related to each other by a fixed ratio this would reduce their (trans-)conductances to one or that ratio. I used the same letters for the renormalized signals, as it is easily visible from the context they are in that they have been renormalized.

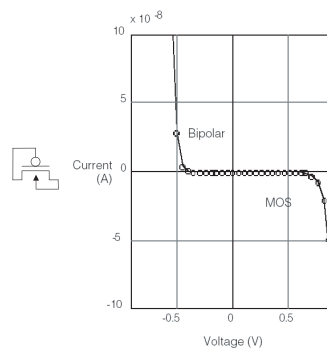


Figure 3: Current-voltage characteristics of the tobi-element. The slope of the curve gives the conductance of the element at any given operating point. The slope and thus the conductance around zero, the expected OP, is very small, thus we expect a big resulting time constant which does not influence the transient behavior of the circuit.

2.4 Analysis of the Self biasing Adaptive Photoreceptor

The classical representation, ignoring miller-capacitances, looks like in figure 1. The transistors are modelled as in figure 4. The output and input capacitances are of parasitic nature and always present. The input capacitance comes from the Photo diode having a relatively large area. The output capacitance comes partly from the feedback path and partly from the output node, which on the chip leads on to the gates of four transistors, each having a considerable amount of capacitance. The bias-capacitance is external and thus can be freely chosen.

The adaptive element in the feedback path (an expansive voltage dependant resistance element with the characteristics as seen in figure 3 called by it's inventor "Tobi"-element) is ignored because it makes the system a fourth order system which is hard to grasp symbolically (also it was not the initial task to consider it and also in the fourth order analysis in chapter 2.7 it has not shown relevant for the stability of the circuit). It is expected to introduce another time constant which is a lot bigger than the other time constants of the circuit, and thus shouldnt influence the circuit in that frequency range and the lower frequency range can not be expected to be exact in the third order approach. The parasitic miller capacitances have been ignored, partially to keep this analysis relatively simple, partially because this model already suffices to demonstrate the transition from a second order system to a third order system. Also drain conductances have been ignored except for the output node, where they compose a high gain amplifier and thus cannot be ignored. We will later see that these simplifications are justified because the model still all the characteristics of the real circuit at least in principle.

One now decomposes the circuit into four parts corresponding to the four time varying voltages (figures 5 - 8). One immediately recognizes that there is a high amount of parameters involved.

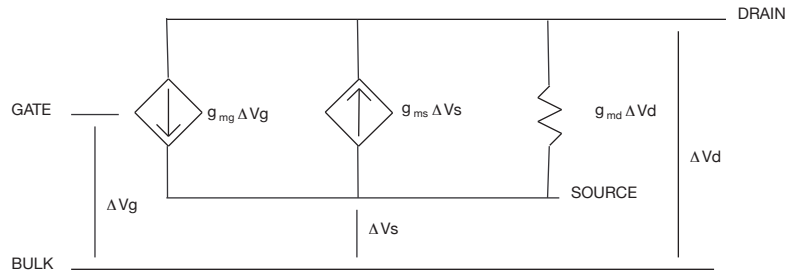


Figure 4: small signal model of the MOSFET transistor

A look at the equation governing the transistor behavior will help simplify this. The widely used equation for subthreshold operation of MOSFET-transistors is:

$$I = I_0 e^{(\kappa V_g - V_s)/U_T} (1 - e^{-V_d s/U_T}) \quad (1)$$

Where κ is the back gate coefficient which covers side effects of effective capacitances between different parts of the transistor (see [2]). In saturation this simplifies to:

$$I = I_{forward} = I_0 e^{(\kappa V_g - V_s)/U_T} \quad (2)$$

Mapping this to the small signal model of the transistor (figure 4) gives us the following expressions for the gate and source conductances:

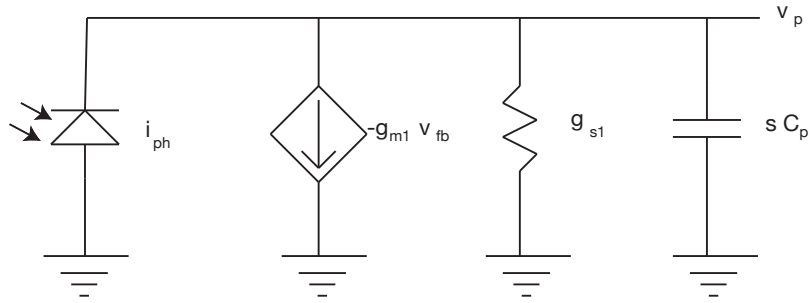


Figure 5: input node

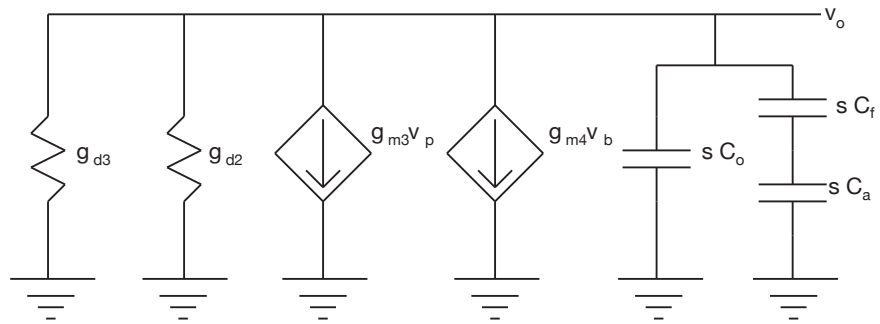


Figure 6: output node

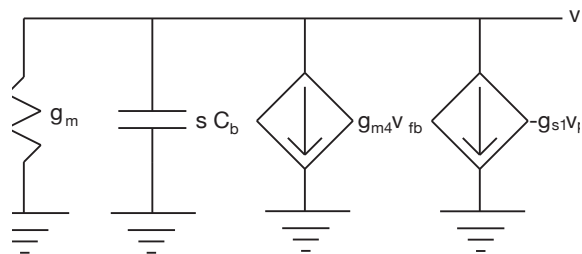


Figure 7: biasing node

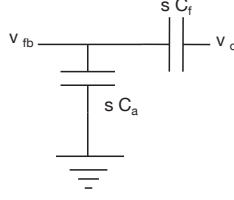


Figure 8: feedback node

$$g_m = \frac{\delta I}{\delta V_g} = \frac{\kappa I}{U_T} \quad (3)$$

$$g_s = \frac{\delta I}{\delta V_s} = \frac{I}{U_T} \quad (4)$$

The equation for the drain conductance is not that obvious, but in reality one observes a finite, approximately constant slope of the current against the drain-source voltage V_{ds} (see also [2]). This can be explained by a change of the active channel length and is usually expressed by the distance from the origin at which a line approximating the saturation-curve crosses the V_{ds} -axis. This distance is called early voltage V_E . From this we have an expression for the drain conductance:

$$g_d = \frac{\delta I}{\delta V_d} = \frac{\kappa I}{V_E} \quad (5)$$

. Now before formulating the equations from the diagrams a lot of simplification can be done in them. First I notice that the diagram for the feedback node involves only two voltages and one kind of element, so it will reduce to a linear relationship between the two voltages:

$$s(v_o - v_{fb})C_f = s v_{fb} C_a \Rightarrow v_{fb} = v_o \frac{C_f}{C_f + C_a} \quad (6)$$

which is then used to substitute v_{fb} out of the other diagrams, leaving us with three diagrams. Second one observes that all conductances scale with the background current, which we know is the photo current background on the left side of the circuit. M_3 and M_4 make up a current mirror mirroring that current to the right side with a fixed factor m depending on the relative geometry of the two. Further we see that most voltages reference relative to U_T . So by multiplying the all equations by $\frac{1}{g_m U_T} = \frac{U_T}{I_p h U_T}$ we effectively reference all voltages relative to the thermal voltage and all currents to the photo current and all remaining parameters are irreducible and dimensionless (figures 9 - 11). Note that the ratios of the capacitances to C_p have been replaced by R_o and R_b respectively (here the effective capacitance of the capacitive network at the output node has been taken for the output capacitance). This leads us to the following set of equations:

$$s\tau_p v_p = -v_p - i_{ph} + A_{cl}^{-1} \kappa v_o \quad (7)$$

$$s\tau_p R_o v_o = -m A^{-1} v_o - m \kappa v_p - m \kappa v_b \quad (8)$$

$$s\tau_p R_b v_b = -\kappa v_b - A_{cl}^{-1} \kappa v_o + v_p \quad (9)$$

Here τ_p is the time constant at the Photo current node, obtained by dividing the input capacitance by the source conductance of M_1 . One is now particularly interested in the natural responses of the system, which in a linear system are given by the eigenvalues and eigenvectors of the matrix of the un driven system. Thus we rewrite equations 7-9 in matrix form:

$$s\tau_p \begin{pmatrix} v_p \\ v_o \\ v_b \end{pmatrix} = \begin{pmatrix} -1 & A_{cl}^{-1} \kappa & 0 \\ -\frac{m}{R_o} \kappa & -\frac{m A^{-1}}{R_o} & -\frac{m \kappa}{R_o} \\ -\frac{1}{R_b} & -\frac{A_{cl}^{-1} \kappa}{R_b} & -\frac{\kappa}{R_b} \end{pmatrix} \begin{pmatrix} v_p \\ v_o \\ v_b \end{pmatrix} - \begin{pmatrix} i_{ph} \\ 0 \\ 0 \end{pmatrix} \quad (10)$$

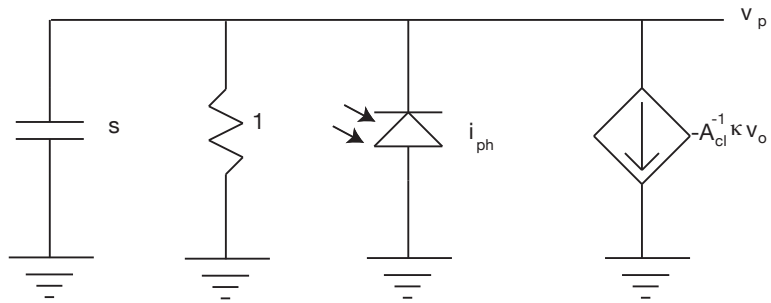


Figure 9: node 1 simplified

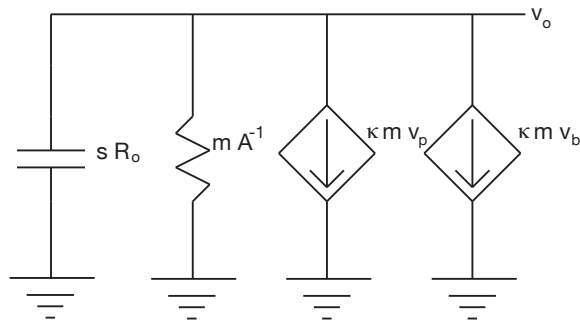


Figure 10: node 2 simplified

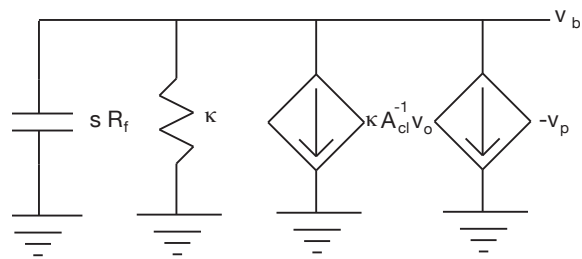


Figure 11: node 3 simplified

The eigenvalues of the homogeneous system are the exponents of the natural responses and at the same time the poles of the transfer function (for obvious reasons) and obviously lead to unstable behavior and/or breakdown of the small signal model in case they have a positive real part. The actual expressions for them are rather messy, so I wont write them here (in the appendix i will include the corresponding Mathematica-notebooks though), but they are numerically available now for given parameter values. One of the results is, however, that most of the time there will be one completely real and Eigenvalue and two which form a complex conjugate pair, which intuitively tells us (as long as the poles are in the left halve of the complex plane) that there will be two cutoff frequencies, one with a 10dB per Octave roll off and one with a 20dB per Octave roll off and the zero can lead to overshoot if it falls in between the two or is smaller (real part which as a rule of thumb approximately determines the position of the corresponding cutoff frequency in the Bode plot) than the smaller one of the two. The transfer function, obtained by solving equations 7-9 is:

$$H(s) := \frac{v_o/U_T}{i_{ph}/I_{ph}} = \frac{A_{cl}(1 + \kappa + R_b s \tau_p)}{\kappa(\kappa + (R_b - 1)s \tau_p) + \frac{A_{cl}}{A}(1 + s \tau_p)(1 + \frac{R_b}{\kappa} s \tau_p)(1 + \frac{A R_o}{m} s \tau_p)} \quad (11)$$

I will rewrite this using the bias- and output-time-constants $\tau_o := R_o \tau_p$ and $\tau_b := R_b \tau_p$:

$$H(s) := \frac{v_o/U_T}{i_{ph}/I_{ph}} = \frac{A_{cl}(1 + \kappa + s \tau_b)}{\kappa(\kappa + s(\tau_b - \tau_p)) + \frac{A_{cl}}{A}(1 + s \tau_p)(1 + s \frac{\tau_b}{\kappa})(1 + s \frac{A \tau_o}{m})} \quad (12)$$

Here one can already see that the ratio of τ_b and τ_p is important. A transition takes place when the capacitances at the input node and the capacitance at the bias node are the same, so I will look now at the three possible cases:

1. $\tau_b > \tau_p$:

In this case for the numerator to be zero its second term has to be negative. Obviously this happens when either one or all three of its factors have negative sign. Only the first case could lead to unstable behavior, because it would lead to a positive pole; it seems from numerical calculations that the second is the case.

2. $\tau_b = \tau_p$:

In this case the circuit is expected to be marginally stable since all poles are negative. Numerical calculations show that it should be only marginally stable, as the overshoot is very big.

3. $\tau_b < \tau_p$:

In this case for a pole to occur the second term has to be positive, which is the case if one or all of its factors are positive, leading to marginal stability or instability.

As one you might have noticed the discussion above doesn't necessarily hold since it doesn't really deal with complex s. Also the zero has not been considered, so one has to be careful if the bias capacitance is small (which will drive the zero into higher frequencies). But I think considering the time frame of this work it is the best that can be done, as it is generally very hard to make intuitive statements about complex polynomials (one only has to look at the exact result for the poles to see what i mean).

What can be done though is use the derived expressions and the more or less known Parameters of the chip to do some numerical calculations. For these calculations i used the following Parameter values

$$A = 100; m = 47; A_{cl} = 9; \kappa = 0.8; R_o = 1 \quad (13)$$

of which most were taken from the chip's geometry (namely those involving capacitance or conductance ratios), one mainly from SPICE-simulations as it cannot be measured directly (the open loop gain A of the output amplifier made from M_2 and M_3) one was extrapolated using the

manufacturers data sheet and the layout file (the Photo capacitance) and one was just straight estimated intuitively considering the layout geometry (the output capacitance). The Results explain the measured step responses (see 3.1) but not the observed instability as according to these calculations the circuit is unconditionally stable.

τ_p was set to unity which effectively sets the scale for the frequency to τ_p^{-1} .

Figure 13 shows a bunch of transfer functions using different ratios R_b . One observes the three

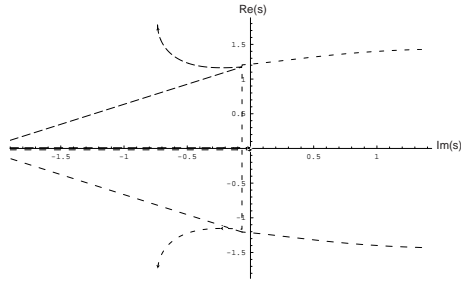


Figure 12: The movement of the zeroes and poles in the s-plane. The zero is the one coming closest to zero. It's always closer to zero than one of the poles which is one condition for stability, the other is that the poles don't have positive real parts, which they don't for $1 < R_b$. The triangle stems from a sudden swapping of places of the poles at $R_b = 1$.

forms, exemplarily shown in figure 13 :

1. When R_b is sufficiently high there are two plateaus one of which has an overshoot and of which the lower frequency one has about double the amplitude. This means that there will be a ringing initial step response to the amplitude of the lower plateau and then a slower rise to the amplitude of the second plateau.
2. As R_b approaches unity the lower plateau vanishes and only one roll off at about 1 takes place. This case is considered ideal as all processes happen with the same speed (ringing, initial gain and final gain) which corresponds to an equal (or near equal) real part of the poles and zeroes of the transfer function. Also this configuration supposedly ([?]) leads to a maximum GainBandwidthProduct (GBP) which basically is a quality measure for an amplifier (Bandwidth normally scales inversely with Gain so the GBP is a constant).
3. With R_b yet becoming less the overshoot shows up again but on the higher level this time spanning up to another magnitude. This in reality has shown to make the circuit unstable which doesn't contradict these result because large resulting signals make the small signal analysis invalid, and the results show that such a large signal can arise out of the small signal model. One could imagine a scenario like this: Resonant behavior leads to a high amount of ringing on the output node around the cutoff frequency, this ringing will cause large current fluctuations in the bias capacitance which is relatively small now so V_b will

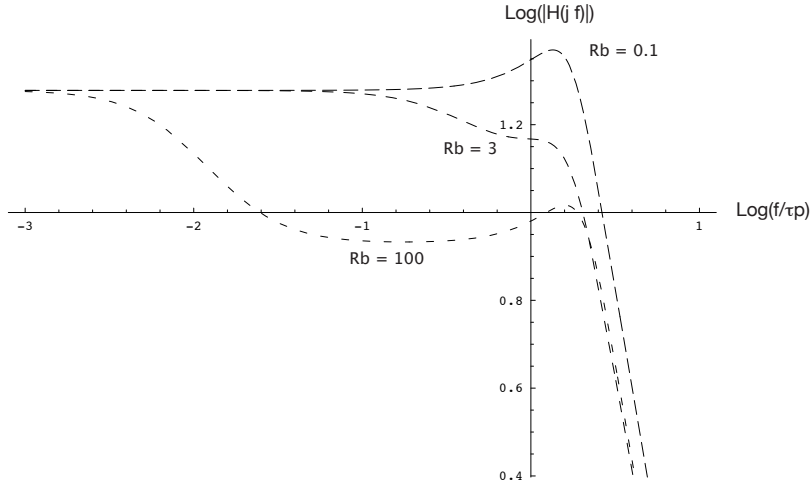


Figure 13: Transfer functions for 3 different Magnitudes of R_b ; the overshoot for high R_b is very small, so it's not visible here. On magnification it shows up on the edge of the lower plateau.

ring loud too which will feedback to the output node via m_3 . If the phase lag of the ringing on the bias node is right these two oscillations while emphasize each other and a resonance catastrophe which results which could lead to limit cycle oscillations f.e..

The optimal setting is the one without overshoot. It corresponds to the poles and the zero lining up on a near common real value, so that the system behaves somewath like a second order low pass. This is the case for the bias capacitance being a couple of times the input capacitance. In the attached notebooks i show that this setting is reasonably save as the positions of the poles an the zero dont change too fast with the parameters.

2.5 Analysis of the Statically Biased Adaptive Photoreceptor

I wont make this discussion as thorough as the one for the self biasing case, as the latter is the actual subject of this article; it is just to point out some differences between the cases.

Static bias means that M_3 and M_4 are no longer connected, the drain of M_1 is hooked to Vdd (positive rail) and M_3 is biased into above threshold to provide for a fast response to suppress ringing (critical damping pushing the zero up to the cutoff of the low pass). In this case the left side and the right side are no longer linked by a current mirror and thus the re normalization done above is less effective. One so obtains the diagram in figure 14. The diagram for the feedback node and the v_p node stay the same and the Diagram for the bias node no longer applies (two effective diagrams for a second order system...).

The resulting matrix is basically the upper left two by two matrix of equation 14 where m is replaced by the ratio of bias- to photo current, which will change as the background illumination changes, thus the transfer function will no longer be self similar as in the self biasing case.

$$sT_p \begin{pmatrix} v_p \\ v_o \end{pmatrix} = \begin{pmatrix} 1 & -A_{cl}^{-1} \kappa \\ \frac{I_{bias}/I_{ph}}{R_o} \kappa & \frac{I_{bias}/I_{ph} A^{-1}}{R_o} \end{pmatrix} \begin{pmatrix} v_p \\ v_o \end{pmatrix} + \begin{pmatrix} i_{ph} \\ 0 \end{pmatrix}. \quad (14)$$

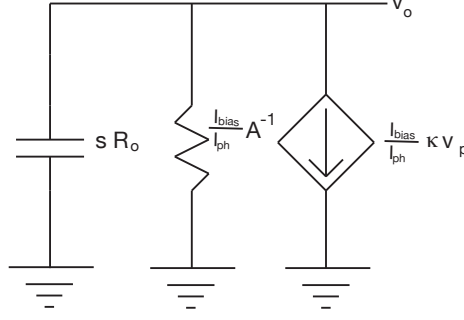


Figure 14: node 2 in the static case

The resulting transfer function is:

$$H(s) := \frac{v_o/U_T}{i_{ph}/I_{ph}} = \frac{A_{cl}/\kappa}{-1 - \frac{A_{cl}}{A\kappa^2}(1 + s\tau_p)(1 + s\frac{A\tau_o}{m})} \quad (15)$$

Second order transfer has been well studied and the canonical form for the transfer function is:

$$H(s) = \frac{A_0}{\tau^2 s^2 + \frac{\tau}{Q} s + 1}. \quad (16)$$

Where τ^{-1} is the common absolute of the Eigenvalues and Q is a measure of the resonance of the circuit. With a high Q there is a high amount of ringing in response to a stepped input. Critical damping, in analogy to a damped pendulum, occurs at $Q = 1/2$. Expansion of the denominator of Eq. 15 and comparison to Eq. 16 yields (here $m := I_{bias}/I_{ph}$):

$$A_0 = \frac{A_{cl}A}{A_{cl}/\kappa + A\kappa}; \quad \tau = \sqrt{\frac{1}{A_0} \frac{R_o}{m\kappa}} \tau_p; \quad Q = \sqrt{A_0} \frac{\sqrt{\kappa R_o}}{1 + \frac{A R_o}{m}}. \quad (17)$$

Solving for the "ideal" $Q = 0.5$ condition gives:

$$Q = \frac{1}{2} \Rightarrow R_o = \frac{m}{A_{cl}A} (A_{cl} + 2\kappa^2 A + 2\kappa \sqrt{\frac{A_{cl}}{A} + \frac{\kappa}{A_{cl}}}) \quad (18)$$

This circuit thus behaves like a standard 2-pole low pass filter but with varying cutoff frequency (τ) and resonance (Q). The corresponding behavior is seen in the step measurements: exponential movement towards the DC-response value and variable amount of Ringing with the frequency of the (variable) cutoff and no self similarity. A more thorough analysis is given in [1].

2.6 Simple source follower photoreceptor

This is the simplest setup possible involving only one transistor and the photo diode. It has the advantage over the other two that it uses a minimal amount of current, even a little less than the self biasing photoreceptor where in order to achieve a high bandwidth the current in the amplifier is a multiple of the photo current, while having a zero-order transfer function with maximum bandwidth and no ringing and no sources for instability. The transfer function in normalized units (which means that the output is contrast encoding as in the other two cases) is unity, as can be read off straight from the diagram, which is already the disadvantage: the above models offer amplification by more than a magnitude.

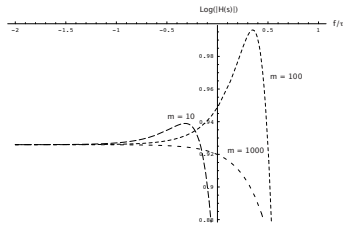


Figure 15: Transfer function of the second order system with varying illumination.

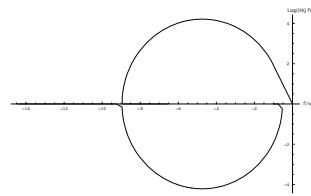


Figure 16: Movement of the poles in the second order system. An explanation of this form has been given in [1].

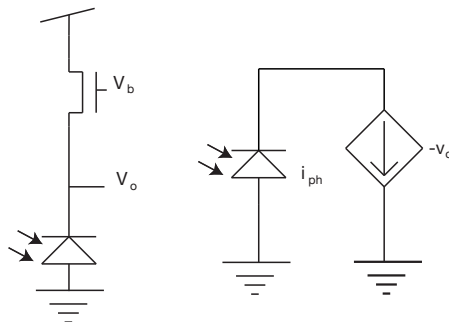


Figure 17: circuit diagram and simplified small signal model for the simple source follower photoreceptor

2.7 Numerical analysis

The symbolic approach breaks down pretty early. already the 3rd order System is hard to grasp, if at all, symbolically, and strictly spoken the intuitive arguments i gave above are derived from the knowledge of looking at the actual resulting Bode plot and the plot of the poles and Zeroes worked out numerically by programs like Mathematica or Matlab.

First i want to go one step further in this "mixed terrain" of symbolical calculations aided

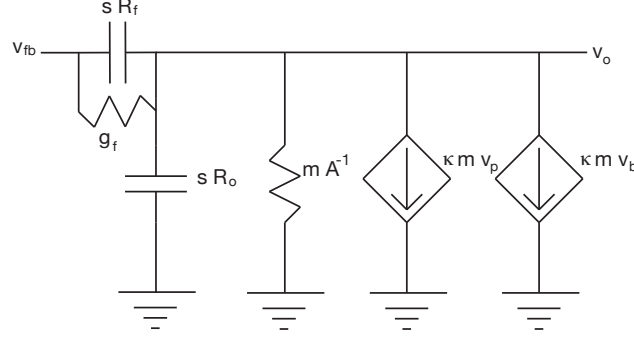


Figure 18: node 2 considering the adaptation

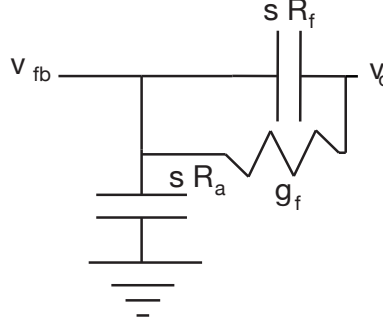


Figure 19: node 4 considering the adaptation

by numerical plotting algorithms by introducing a 4th order approach. The 4th order comes in when one doesn't neglect the conductance of the feedback path which is responsible for the adaptation. The diagram for the output node and the feedback node change as in figures 18 and 19. The other two diagrams only change in that $A_{cl}^{-1}v_o$ is replaced by v_f . A_{cl}^{-1} is no longer explicitly used, since the capacitors that form it are considered explicitly instead. The system of equations for this is:

$$s\tau_p v_p = -v_p - i_{ph} + \kappa v_f \quad (19)$$

$$s\tau_p R_o v_o = -mA^{-1}v_o - m\kappa v_p - m\kappa v_b - (sR_a\tau_p + g_a)(v_o - v_f) \quad (20)$$

$$s\tau_p R_b v_b = -\kappa v_b - \kappa v_f + v_p \quad (21)$$

$$s\tau_p R_f v_f = (sR_a + g_a)(v_o - v_f) \quad (22)$$

They still fit on one page, the solution doesn't and looking at it ceases to be very illuminating.

The transfer function (figure 21) predicts a bandpass behavior of the circuit. The interpretation is that a new pole/zero pair is introduced which delivers a high pass cutoff which indicates the insensibility (or adaptivity) to a DC background, as it is strongly diminished in the Bode plot which is not surprising at all.

Originally the adaptation conductance supplied by the tobi element was thought to be fixed but it then turned out that due to insufficient guarding it would scale with light intensity as the rest of the circuit. This mistake should now give us a mostly invariant transfer function and thus step response if rescaled by the light intensity!

Above this new cutoff the transfer function remains principally the same and the same three forms as in the 3rd order analysis are obtained. The poles and zeroes, as shown in 20 move much like in the third order model. An additional zero is present representing the high pass cutoff which is not visible in the plot because it is stationary. The ringing now depends strongly on how big the capacitors in the feedback path are: big capacitors will suppress ringing. Basically this shows us that our neglecting the adaptation was noncritical, as we knew about the adaptation before, and now we know that considering it doesn't bring any new unexpected predictions.

Simulations using circuit simulators based on linear models much like the ones used but

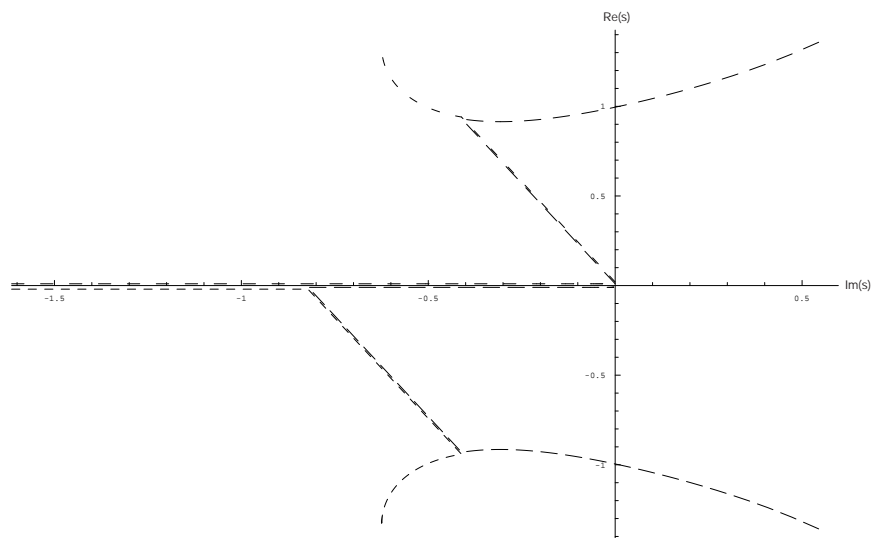


Figure 20: Poles and zeroes of the 4th order system

including all parasitic side effects have been done a lot to gain intuition for the circuit. They present mostly the expected behavior that is also seen in reality. One has shown instability which has also been observed on the chip with a small bias capacitance and under low illumination and which is generally predicted by the models i used for low biasing capacitances, but it is unclear as to how far these simulations can be trusted.

2.8 Predictions for Stability and optimal tuning

The motivation behind the work presented in the last chapters, which represents the core of my efforts in this semesterarbeit, is to find answers to the two questions:

1. Under what circumstances can the circuit expected to be stable?
2. What recommendations can be extracted from the model for an optimal tuning of the parameters?

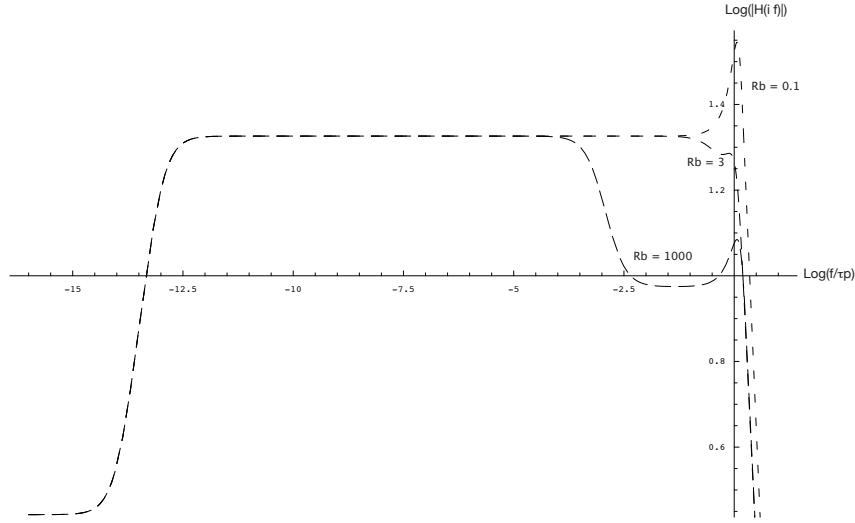


Figure 21: Transfer of the 4th order system

The first question is easy to answer. The plots of the movement of the poles and zeroes of the transfer functions obtained from third and fourth order small signal analysis show that the poles have positive real parts and thus an unstable exponentially growing natural response for too small values of the biasing capacitance C_b . The zeroes are non critical since their real parts are always smaller than the real part of at least one pole.

The second question could not be answered as clearly as hoped. It is generally expected and also can be observed in the evolution of the transfer function with changing biasing capacitance, that a solution with minimal ringing is obtained when the poles and zeroes are maximally aligned, meaning their real parts are as close to each other as possible. Dues to the complexity of the equations no closed form for this condition could be found, but the results show such an alignment for a biasing capacitance which is a couple of times the capacitance of the photodiode. Care has to be taken here because the biasing capacitance on the chip is connected to the whole array of photoreceptor, so it effectively has to be divided by the number of photodiodes it is feeding before it is entered into the (single-receptor) model. Thus for the chip a capacitance of about $7 * 3 * 1.4nF = 29.4nF$ should be optimal (the capacitance of 1.4 nF for the photodiode has been calculated from its area and the process specification data sheets).

The analysis also shows that an optimal setting, once obtained for one illumination should be valid for all illuminations as the transfer function remains the same when subjected to renormalization!

2.9 Noise

In [1] the following well known noise model has been verified to be applicable to this circuit:

$$\frac{di^2}{df} = 2qI \quad (23)$$

In the models derived in the last chapters for the self biasing photoreceptor a renormalization has been applied where currents are taken relative to the average Photocurrent, voltages to the thermal voltage and time scales relative to the RC time constant of the input node which in turn scales with Illumination (because the conductance of the feedback transistor scales with current).

Thus in the above equation I scales linear with Illumination while f scales inversely and q only depends on the thermal voltage which is the unit for the voltage and thus the charges on the capacitors. Since the total bandwidth of the transfer function when subjected to renormalization is expected to be invariant the total noise power is also expected to be invariant under changes of background illumination (the renormalization applies on both sides of eq. 23!) and only dependant on the thermal voltage and thus on the temperature with which it is expected to increase.

3 Measurement

3.1 Stepresponses

3.1.1 Static bias

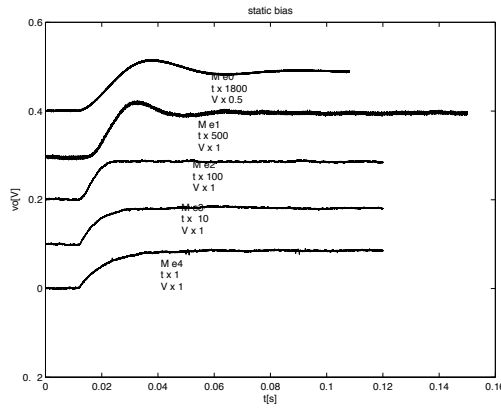


Figure 22: step response of the statically biased photoreceptor

In figure 22 you can see the step response of the statically biased circuit under different illuminations. They are not self similar. Neither the amount of ringing nor the bandwidth scale linear with intensity. Also one can see that ringing is not fully suppressed. It is probably rather impossible to do this for all illuminations, as important parameters change with illumination.

3.1.2 Adaptive Bias

In figure 23 you can see the step response of the self biasing circuit. They are absolutely self similar at least on the onset, the amplitude of which corresponds to the first plateau of the transfer function for intermediate bias capacitances. The slight increase of amplitude with intensity can be interpreted as contrast diminution by the used filters. The time scale scales nearly linear. There is about one magnitude change in time scale per magnitude change in illumination. Again the deviation can be explained by imperfections of the used filters.

In the step responses one observes an increasing amount of noise, while the model predicted a constant noise over all ranges of illumination. I ascribe this additional noise to the feedback node. When one derives the equation for the capacitive divider one silently drops any subsident

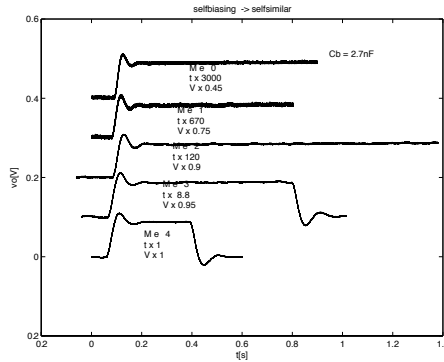


Figure 23: step response of the self biasing photoreceptor

dc charge on the capacitors. In reality this charge is a representation of the dc background illumination the circuit has adapted to, thus it will be larger for stronger illuminations which in turn will increase the noise as follows from equation 23.

3.2 Transfer function

Figure 24 shows the actual transfer functions of the self biasing circuit under different illuminations. A slight decrease in relative bandwidth is observed which is not observed in the theory. Also an additional overshoot on the adaptation cutoff increasing as the intensity decreases is visible. This has been observed in simulations but not in the theory up to fourth order. Since the instability also first shows in the simulation, and since the overshoot increases with decreasing light intensity, which was also in reality what made the instability more probable, this feature is likely to be linked to it. It seems somehow similar to the overshoot showing up in the second order system where also it was impossible to perfectly tune the circuit because elements didnt scale with illumination, so it is expected that it originates from side effects which do not exhibit scaling with intensity, possibly the conductance of the feedback path and miller capacitances whose effective size can depend on the response speed of the circuit (possibly resulting in a quadratic and not linear scaling with intensity).

3.3 Power consumption

measured power consumption:

9V direct battery power (no regulator):

all functionality enabled, chip uses 1mA

turning off follower pads:

with photoreceptor self biasing 100uA

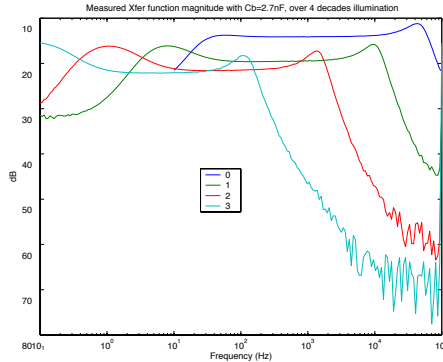


Figure 24: measured transfer of the self biased photoreceptor

with static 10uA bias on each receptor 150uA

The power consumption of a single circuit in self biasing mode is comparable to the power consumptions of the rod in the eye as shown in [1]. Thus the aim of reconstructing a biological vision cell has partially already been achieved as in the power consumption, contrast encoding, high gain and ability to sense even single photons; the latter is the main advantage of the constant integration mechanism utilized here (charges are collected all the time, adaptation takes place over a relatively long time scale) over sampling mechanisms like CCDs as discussed in [1].

4 Conclusion

In this paper the additional complications due to a small expansion to a small circuit has been studied. It turned out that while showing very desirable features such as self similar step responses which allow for optimal tuning and low power consumption comparable to biological counterparts maintaining an efficiency which is also comparable (single photon integration), the new design exhibits a much higher degree of complexity and unpredictability. Especially the fact that contributions of higher order than the fourth, which is already so complex that it cannot be understood without numerical calculations, have a significant effect is somewhat shocking and discouraging.

Still i do not consider this work a failure. In my opinion it nicely shows exactly this transition from simple, easy to understand intuitively circuits to more complex systems that quickly leave the realm of intuition tending to break out of the intuitive picture one has just come to after large amounts of thinking. Thus one is forced not to rely on one technique but to acquire a robust set of techniques including algebraic linear analysis, numerical calculations and simulations and advanced measurement techniques such as automated spectrum analysis. One is

forced to immediately test and compare any results obtained using one technique against the others otherwise risking wasting a lot of time.

Sticking with this paradigm the task of understanding a circuit such as this becomes less horrible and one slowly gains a higher degree of intuition based on the sum of the different approaches. I also found that it was very important to keep having feedback on the obtained results, models and intuitions as I tended to stick to one that would exhibit a certain elegance and simplicity but that would break down under more objective examination.

Finally, I consider this work a success in the sense that it gave me a deep insight into the matter of AVLSI and after quite some frustration with pages of equations i came back to seeing the beauty of dynamic systems (it is worth considering at this point what a digital machine could do with, say, five gates, already including more elements than this circuit), and AVLSI has lost much of its enigmatic appearance to me that it had before and the techniques i learned make the idea for example of designing such circuitry less utopic.

References

- [1] Tobi Delbrueck and Carver A. Mead. Analog vlsi phototransconduction. *CNS Memo*, (30):23, April 1996.
- [2] Liu, Kramer, Indiveri, Delbrueck, and Douglas. *Analog VLSI: Circuits and Principles*. MIT Press
Cambridge, Massachusetts
London, England, 2002.